SCREEN UTILITY SIMULATION - EXPLAINING THE EVOLUTION AND FUTURE OF SCREEN PRINTED METALLIZATION OF SI-SOLAR CELLS

S.Tepner[a)*], L.Ney[a)], M.Singler[a)], M.Linse[a)], A. Lorenz[a)], M. Pospischil[a)], F. Clement[a)] and R.Preu[a)]

a) Fraunhofer Institute for Solar Energy Systems ISE, Heidenhofstraße 2, 79110 Freiburg, Germany
*Corresponding author: Sebastian Tepner | Phone: +49 (0)761 4588 4074 | e-mail: sebastian.tepner@ise.fraunhofer.de

ABSTRACT Flatbed screen printing is still the dominant metallization technique for Si-solar cells because it proved to be reliable and cost effective while maintaining to be innovative. The latest reductions of printed Ag-electrode width in the range of 20 µm were mainly driven by further screen optimization. Screen printing pastes have evolved accordingly in order to maintain sufficient contacting behavior at narrow line widths. Our previously published screen simulation model allows to create a virtual representation of any screen opening based on the common screen parameters mesh count, wire diameter, screen angle and opening width. In this work, we discuss its implication by establishing the dimensionless parameter screen utility index SUI which quantifies the compromise between screen stability and opening structure for a sufficient printability. We further show how this parameter has evolved over the last decade for printing experiments conducted at Fraunhofer ISE and discuss what challenges this trend will create for the future of screen printed metallization. Finally, we combine requirements for screen tension, screen utility and reproducibility of finger geometry by applying the deviation of the screen opening rate in a single diagram to visualize the trade-off regarding future screen design.

1 MOTIVATION

Flatbed screen printing remains the dominant metallization process with over 97% market share [1]. Over the last 20 years, there has been tremendous progress in reducing the printed Ag-electrodes width (referred to as fingers width). In 2007, Mette reported finger width of around 100 µm [2] which have been further reduced by approximately 6-8µm per year until Clement et al. presented finger widths of 22 µm at the last EU PVSEC in 2019 [3]. Later during that year, Tepner et al. was able to demonstrate finger widths of only 19µm at an aspect ratio of over 0.9 [4,5]. These achievements were mainly driven by paste and screen optimization [6]. Especially the later, plays a critical role when a further optimization of the paste transfer is desired. Over the last years, different research studies investigated the correlation between the screen geometry and printing results [7–12]. Furthermore, Riemer et al. [13,14], Kapur et al. [15], and Taroni et al. [16] contributed significantly to the understanding of paste transfer by modeling attempts of the flatbed screen printing process. However, these models discuss flooding of meshes rather than transferring the paste through full screen architectures. In order to further progress on the later, we have published a screen simulation model which allows the exact calculation of the entire geometric structure of a screen opening based on the common screen specification parameters [17,18]. Figure 1 presents an overview on the definition of a regular finger opening on a screen used in flatbed screen printing for solar cell metallization. The underlying mesh is defined by the mesh count MC, therefore the wire-to-wire distance d_0 and the wire diameter d. On top, an emulsion layer is placed at a certain screen angle φ. The screen opening width w_n finally defines a set of individual openings with a specific shape and area. In previous work, we have studied what type of individual openings shapes exist and how its frequency of occurrence changes with different screen parameters. Throughout this work, we present the latest findings around that topic by advancing the theoretical description of that screen opening structure. We will first summarize our key findings and then introduce a novel dimensionless parameter which helps to quantify the screen utility in terms of its expected printability for a given printing medium (e.g. metal paste).

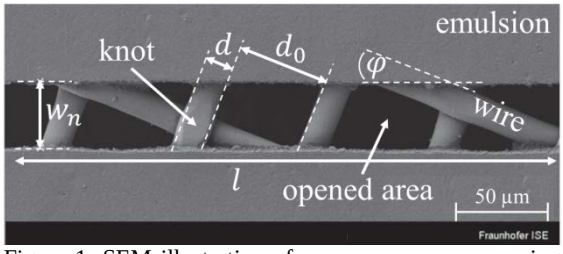

Figure 1: SEM illustration of a common screen opening defined by the underlying mesh (mesh count MC and wire diameter d), screen angle φ and opening width wn.

2 SCREEN SIMULATION MODEL & THEORY

Figure 2 presents the virtual representation of a common screen opening. Our previously published mathematical screen model allows the creation of arbitrary screen opening channels by using the four key specification parameters mesh count MC, wire diameter d, screen angle φ and opening width w_n [17]. Based on these parameters the average opening rate is calculated by equation 1.

$$OA_{\%} = \frac{{d_0}^2}{(d + d_0)^2} \qquad \text{Eq. (1)}$$

The wire-to-wire distance d_0 is calculated by equation 2, respectively.

$$d_0 = 1 / MC - d \qquad \text{Eq. (2)}$$

The opening rate $OA_{\%}$ is an established parameter in industry, indicating the magnitude of possible paste transfer during screen printing. However, equation 1 only grants the average value across in infinite long screen opening channel. In previous work we have introduced the average standard deviation of this parameter across the channel length l as shown in equation 3. By analyzing

this parameters, we were able to demonstrate that the screen angle plays a major role when a further optimization of the screen opening structure is desired [17].

$$\sigma_{OA} = \sqrt{\frac{1}{n_y}\sum\left(A_{Ind.Opening} - \overline{OA_{\%}}\right)^2} \qquad \text{Eq. (3)}$$

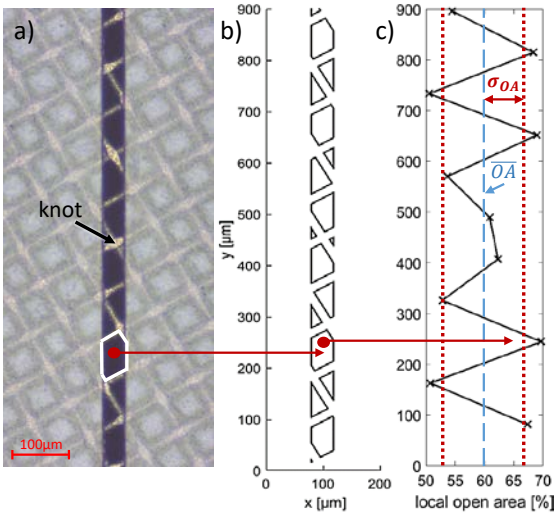

Figure 2: Virtual representation of a screen opening with a mesh count MC 360 1/inch, a wire diameter d = 16 µm, screen angle φ = 30° and an opening width of w_n = 40 µm. Fraunhofer ISE developed a simulation tool which allows the creation of any virtual screen opening. a) Microscope image of a 360/16/30° screen with a screen opening w = 40 µm. b) Geometric presentation of a virtual screen with the same properties. c) Local open area varying along the screen opening length l with $OA_{\%}$ = 59.79 % and σ_{OA} = 6.89 %.

Furthermore, the screen tension is a crucial parameter for reproducibility, screen lifetime and snap-off mechanics. The maximal obtainable screen tension γ_{screen} (calculated by equation 4) is an important parameter when it comes to evaluating the above.

$$\gamma_{screen} = \frac{\pi}{4} \cdot \sigma_{uts} \cdot MC \cdot d^2 \qquad \text{Eq. (4)}$$

The parameter σ_{uts} gives the ultimate tensile strength of the corresponding wire material.

3 RESULTS & DISCUSSION

A closer look at equation 1, 3 and 4 gives rise to a classical optimization problem. What type of mesh will be the best compromise between screen lifetime, fast and reproducible screen snap-off and a sufficient homogenous opening structure for a desired screen opening width w_n?
In order to combine the opening structure with the obtainable screen tension, we present in [5,19] a novel dimension parameter which allows to quantify the presented trade-off. Equation 5 presents the screen utility index SUI which is calculated by the ratio between the average individual area of openings and the average area of a blocking wire. This ratio is further multiplied by the term $\cos(\varphi)^{-1}$ in order to account for the angle dependency of the number of mesh units contributing to the screen opening.

$$SUI = \frac{\overline{A_{Ind.Opening}}}{\cos\varphi \cdot d \cdot d_0} \qquad \text{(Eq.5)}$$

The question emerges what values for the screen utility index one should aim for when designing a screen. Taking a look at the special case when SUI = 1 applies, equation 5 reveals that the area of individual openings match the area of blocking wire elements including the scale of additional mesh units at increasing screen angles by multiplication of the term $\cos(\varphi)^{-1}$. If the designed screen has a SUI < 1, the underlying mesh is too coarse for the corresponding opening structure, limiting the paste transfer. On the other hand, when SUI > 1 applies, the chosen screen opening w_n will result in sufficient average area of individual openings for the chosen underlying mesh. However, these statements neglect clogging of individual openings by rigid particles within the printing paste. In order to account for a sufficient printing with state of the art Ag front-side pastes, one should aim for a SUI > 1.5 [19]. In Figure 3, we present accumulated data from printing experiments at Fraunhofer ISE over the last ten years, demonstrating the evolution of the screen utility index for screens with a state of the art screen angle of φ = 22.5°. Only in recent time, we challenged the screen printing process to the point where usual screen architectures fail completely. This result highlights the need for a novel approach to further optimize the screen design.

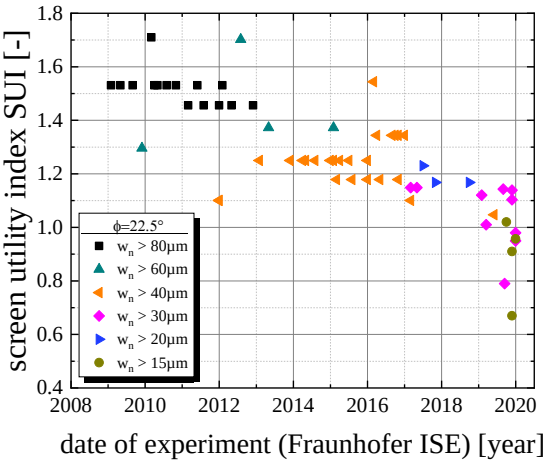

Figure 3: Evolution of the screen utility index at Fraunhofer ISE over the last decade. A clear trend towards smaller values of the SUI emerges, revealing that the demand for small screen openings was evolving too fast for the evolution of fine meshes. The industry should push the development for the finest meshes possible in order to maintain a sufficient screen utility index.

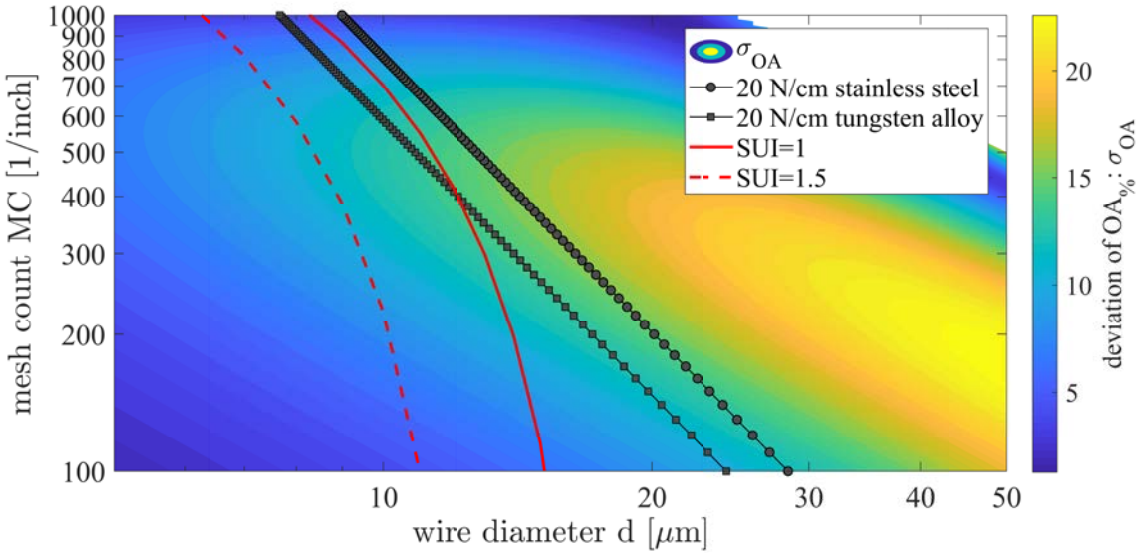

Figure 4: Dependency of the standard deviation of the opening rate σ_{OA} on the type of mesh is presented for mesh counts between 100 – 1000 1/inch and wire diameters between 5 – 50 µm. The screen architecture is chosen by using a screen opening width w_n = 20 µm and a screen angle φ = 22.5°. Furthermore, constant values for screen tension γ_{screem} = 20 N/cm for stainless steel and tungsten wires are given. The minimum screen utility index for a sufficient opening structure SUI = 1 and the optimal screen utility for PERC metal pastes SUI = 1.5 are shown.

Figure 4, presents a combination of all presented aspects of screen design in a single diagram. The average deviation of the opening rate σ_{OA} is shown for meshes with mesh counts ranging from MC = 100 – 1000 1/inch and wire diameters ranging from d = 5 – 50 µm. Furthermore, screen tension data for γ_{screen} = 20 N/cm for stainless steel and tungsten wires are given. Finally, constant lines for the screen utility index are shown. Here, a screen architecture of a regular φ = 22.5° is shown for a screen opening width of w_n = 20 µm is assumed. The ITRPV 2020 indicates that in the upcoming years a stable, reliable and fast screen printing process for printed finger widths of w_f = 25 µm is expected [1]. When taking into account that a fast printing ultimately leads to significant shearing of metal pastes and subsequently paste spreading on the silicon wafer in the range of a couple of micrometers [11], the goal of establishing 20 µm screen openings for screen designs is even conservative. The data in Figure 4 suggests that state of the art meshes are barely equipped to fulfill this trade-off between screen tension and sufficient screen utility index. Taking into account, the clogging tendencies of current metal pastes with Ag-particle sizes in the range of 2-4µm [9], the empirical requirement for the SUI = 1.5 cannot be met. Current meshes with mesh counts of 480 or 520, made out of tungsten wires with a diameter of d = 11 µm are only fine enough for printing finger width in the regime of 20 µm at low printing speeds because at such speeds significant spreading can be prevented. To further precede the evolution of screen printing metallization, we suggest that new wire materials with increased ultimate tensile strength are invented in order to significantly reduce the corresponding wire diameter without compromising screen stability. The next generation of wires should have a diameter not bigger than 8.8 µm in order to meet the requirements for a fast, reproducible screen printing at the 20µm level. Other ways of optimizing the screen utility index by e.g. changing the screen angle have been studied by us extensively [5,18,19].

4 SUMMARY AND OUTLOOK

This work presents an approach on how the evolution of screen printing for solar cell metallization can be put into a quantitative context regarding screen design. A screen is a geometric object which creates a unique opening structure depending on the common screen parameters. In order to print fine lines through such a screen, a sufficient rate of individual openings must be maintained. On the other hand, the screen itself needs to have a minimum stability, requiring a certain ratio between numbers of wires per unit length and wire diameter. In this work, we present the dimensionless parameter screen utility index which quantifies the potential compromise between these aspects. We further show the evolution of this parameter for experiments conducted at Fraunhofer ISE since 2009, revealing that the industry demands reduction of finger width faster than mesh development can keep up with. More recently, we have challenged the screen printing process by printing through screen openings of only 15µm on screens made out state of the art meshes [5]. Results indicate that current wire diameters are too big for ultra-fine screen printing. Finally, we combine the requirement for the screen utility index with requirements for screen tension to show that a revolution on wire materials is needed in order to comfortably push fine line screen printing into the sub 20 µm range for printed structure size.

5 ACKNOWLEDGEMENT

The authors thank all colleagues at Fraunhofer ISE for valuable discussions on the presented topic. Further, the authors thank all partners from industry around screen printing for their insights.

6 REFERENCES

1. International technology roadmap for photovoltaic. 11th edition: 2019 Results. *ITRPV* 2020.
2. Mette A. *New Concepts for Front Side Metallization of Industrial Silicon Solar Cell*; 2007.
3. Clement F, Linse M, Tepner S, Wengenmeyr N, Ney L, Krieg K, Lorenz A, Pospischil M, Bechmann S, Oehrle K, Steckemetz S, Preu R. "Project FINALE" - Screen and Screen Printing Process Development for Ultra-Fine-Line Contacts below 20µm Finger Width. *36th EU PVSEC Conference Proceedings* 2019: 259–62, DOI: 10.4229/EUPVSEC20192019-2DO.5.1.
4. Tepner S, Ney L, Linse M, Lorenz A, Pospischil M. Advances in Screen Printed Metallization for Si-Solar Cells – Towards Ultra-fine Line Contact Fingers Below 20 µm. *29th International PV Science and Engineering Conference, Xi´an, China* 2019, DOI: 10.13140/RG.2.2.33088.69126.
5. Tepner S, Ney L, Linse M, Lorenz A, Pospischil M, Masuri K, Clement F. Screen Pattern Simulation for an Improved Front-Side Ag-Electrode Metallization of Si-Solar Cells. *Prog. Photovolt: Res. Appl.* 2020, DOI: 10.1002/pip.3313.
6. Tepner S, Wengenmeyr N, Ney L, Linse M, Pospischil M, Clement F. Improving Wall Slip Behavior of Silver Pastes on Screen Emulsions for Fine Line Screen Printing. *Solar Energy Materials and Solar Cells* 2019; **200**: 109969, DOI: 10.1016/j.solmat.2019.109969.
7. Thibert S, Jourdan J, Bechevet B, Chaussy D, Reverdy-Bruas N, Beneventi D. Influence of silver paste rheology and screen parameters on the front side metallization of silicon solar cell. *Materials Science in Semiconductor Processing* 2014; **27**: 790–9, DOI: 10.1016/j.mssp.2014.08.023.
8. Fortu Z, Song LX. Identifying Screen Properties to Optimise Solar Cell Efficiency and Cost. *Energy Procedia* 2013; **33**: 84–90, DOI: 10.1016/j.egypro.2013.05.043.
9. Yüce C, König M, Willenbacher N. Rheology and Screen-Printing Performance of Model Silver Pastes for Metallization of Si-Solar Cells. *Coatings* 2018; **8(11)**: 406, DOI: 10.3390/coatings8110406.
10. Xu C, Willenbacher N. How rheological properties affect fine-line screen printing of pastes: A combined rheological and high-speed video imaging study. *J Coat Technol Res* 2018; **15(6)**: 1401–12, DOI: 10.1007/s11998-018-0091-2.
11. Tepner S, Wengenmeyr N, Linse M, Lorenz A, Pospischil M, Clement F. The Link between Ag-Paste Rheology and Screen Printed Metallization of Si Solar Cells. *Adv. Mater. Technol.* 2020, DOI: 10.1002/admt.202000654.
12. Abdel Aal K, Willenbacher N. Front side metallization of silicon solar cells – A high-speed video imaging analysis of the screen printing process. *Solar Energy Materials and Solar Cells* 2020; **217**: 110721, DOI: 10.1016/j.solmat.2020.110721.
13. Riemer DE. Analytical Engineering Model of the Screen Printing Process: Part 1. *Solid State Technology* 1988; **Nr. 8**: 107–11.
14. Riemer DE. The Theoretical Fundamentals of the Screen Printing Process. *Microelectronics International* 1989; **6(1)**: 8–17, DOI: 10.1108/eb044350.
15. Kapur N, Abbott SJ, Dolden ED, Gaskell PH. Predicting the Behavior of Screen Printing. *IEEE Trans. Compon., Packag. Manufact. Technol.* 2013; **3(3)**: 508–15, DOI: 10.1109/TCPMT.2012.2228743.
16. Taroni M, Breward CJW, Howell PD, Oliver JM, Young RJS. The screen printing of a power-law fluid. *Journal of Engineering Mathematics* 2012; **73(1)**: 93–119, DOI: 10.1007/s10665-011-9500-6.
17. Ney L, Tepner S, Linse M, Lorenz A, Bechmann S, Weber R, Pospischil M, Clement F. Optimization of Fine Line Screen Printing Using in-depth Screen Mesh Analysis. *AIP Conference Proceedings* 2019: 20006, DOI: 10.1063/1.5125871.
18. Tepner S, Ney L, Linse M, Lorenz A, Pospischil M, Clement F. Studying Knotless Screen Patterns for Fine Line Screen Printing of Si-Solar Cells. *IEEE J. Photovoltaics* 2020; **10(2)**: 319–25, DOI: 10.1109/JPHOTOV.2019.2959939.
19. Tepner S, Ney L, Singler M, Preu R, Pospischil M, Clement F. Generalization of Screen Utility in Fine Line Screen Printing – A Method to Predict the Future of Si-Solar Cell Metallization. *Scientific reports* 2020.